

THERMAL SIMULATION OF ELECTRICAL HEATING OF SHAPE MEMORY ALLOYS WIRES INTO A POLYMERIC MATRIX WITH TWO DIFFERENT SEQUENCES OF ACTIVATION

Lorena Monteiro Cavalcanti Barbosa, asukamonteiro@yahoo.com.br

Celso Rosendo Bezerra Filho, celso@dem.ufcg.edu.br

Carlos José de Araújo, carlos@dem.ufcg.edu.br

Rômulo Pierre Batista dos Reis, soromulo@hotmail.com

Federal University of Campina Grande, Center of Science and Technology, Department of Mechanical Engineering, ZipCode 58429-900, Campina Grande, Paraiba, Brazil

Abstract. *The shape memory materials have attracted great interest in various fields of applications because of their special functional. Among the smart materials, the shape memory alloys (SMA) are the best representatives of the class of metals. In this context, Ni-Ti SMA are the most successful smart metals today because combine good functional properties with a high mechanical strength. The electrical resistivity of Ni-Ti is high enough for direct Joule heating by passing an electrical current. In this sense, this paper aims to show the results from a numerical simulation of the temperature distribution as a function of the electrical current and of the time, for an structure composed of Ni-Ti SMA wires embedded into a polymeric matrix, when different wires are turned on and compare the results of two different activations, using the ANSYS CFX software. Results of behavior the distribution temperature along time, line and contour lines were analyzed. Through of results, it is revealed the influence of quantity of turned on wires, and position of wires turned on for the distribution temperature.*

Keywords: *Shape Memory Alloys, Joule heating, Ni-Ti, CFX, Active Composites*

1. INTRODUCTION

The shape memory materials have attracted great interest in various fields of applications such as aerospace, robotics, structural applications and civil engineering. Due to of their special functional properties, known as the shape memory effect (SME) and superelastic effect (SE) (Urbina, *et al* 2010). Many alloys displaying shape memory have been found and considerable effort is still being made to discover new materials (Huang, 2002; Savi *et al.*, 2002; Ashrafiuon *et al.*, 2006).

The shape memory alloys (SMAs) are able to “remember” a geometrical shape at high temperature and another shape at low temperature, and during the repeated heating and cooling the SMAs change its shape between these two shapes without the help of the external stress (Meng *et al.*, 2004).

The use of SMA is a major scientific and technological challenge in the area of smart materials and structures. Currently there is a very large variety of materials presenting the SMA phenomenon. However, only have commercial interest those with a significant shape recovery or that offer considerable recover forces when restricted to recovering its original shape after the imposition of temperature, and its properties are strongly dependent on alloy composition (Van Humbeeck, 2001; Chen, *et al.*, 2009; Kang *et al.*, 2011)

NiTi shape memory alloys (SMAs) are the most successful shape memory alloys today because they combine good functional properties with a high mechanical strength (Frenzel *et al.*, 2004).

The resistivity of Ni-Ti is high enough for direct Joule heating by passing an electrical current. This is an additional advantage as the actuation of Ni-Ti shape memory alloy based devices is simplified. In term of the size of Ni-Ti shape memory alloys in engineering applications, one can see a quick movement in recent years from large size (An *et al.*, 2008; Frenzel *et al.*, 2011). There are many investigations on the effect of ternary alloying elements such as Cu, Fe, Nb, Mo, Hf, etc. on phase transformation behavior, SME and superelasticity in TiNi SMAs (Li *et al.*, 2005).

The structure to be studied in this work is a Shape Memory Alloy Hybrid Composite (SMAHC) designed as an active beam of epoxy resin that contains five Ni-Ti pre-trained wire actuators, uniformly distributed along its neutral plane. These SMA wires can be activated differently and controlled by resistive heating (Joule effect).

In this sense, this paper aims to show results from numerical simulation of the temperature distribution as a function of the electrical current, when different wire are driven, and to compare the results of two different activation.

2. MATERIAL AND METHODS

2.1 The SMAHC Beam

The system in analysis is a SMAHC beam with 300 x 24 x 4 mm, with SMA wires of 0.29 mm in diameter and 300 mm in length. Figure (1) shows a schematic drawing of SMAHC.

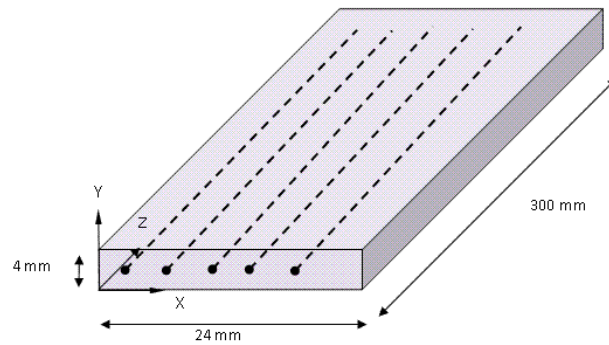


Figure 1. The SMAHC beam with Ni-Ti wires

Figure (2) shows how the wire Ni-Ti was driven. In this work two different activations were done. Activation mode 1 when two wires are turned on with the setup shown in Fig. (2) and activation mode 2 for three wires turned on. These trained Ni-Ti wires, when heated electrically tends to shrink inside the composite. In this paper this effect will not be considered.

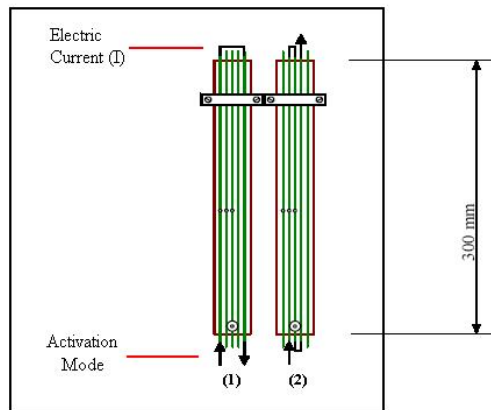


Figure 2. Electrical activation for Ni-Ti wires

The Ni-Ti wires are driven by an electrical current that varies linearly with time from 0 to 1.5 A between 0 to 145 seconds in the heating, and from 1.5 A to 0 for 145 to 260 seconds during cooling. How is describes by Eq. (1).

$$I(t) = \begin{cases} \frac{1,5t}{145} & \text{to } 0 \leq t \leq 145 \\ -\frac{1,5t}{115} + \frac{390}{115} & \text{to } 145 < t \leq 260 \end{cases} \quad (1)$$

Propriety of the SMAHC and the Ni-TI wires are consider constant and shown in Tab (1).

Table 1. Material properties of epoxy resin and Ni-Ti wires.

Properties	Epoxy	Ni-Ti Wire
Density (g/cm ³)	1.18	6.48
Reference Pressure (atm)	1	1
Reference Temperature (°C)	24	24
Resistivity (μΩ.m)	-	85

Thermal Conductivity (W/m.K)	0.4	8.5
Specific Heat (J/kg.K)	1050	400

2.2 Methodology Computational

Commercial software *CFX 5.6* was used to simulate the conduction heat when wires were electrically activated. The tri-dimensional model employed comprises the energy conservation equation in three directions.

A transient model was used with time step of 1s for a time total of 260s, and a convergence criterion of 10^{-8} . The mesh was built in *CFX-Build*. Figures (3) and (4) show the volume distributions in the computational domain.

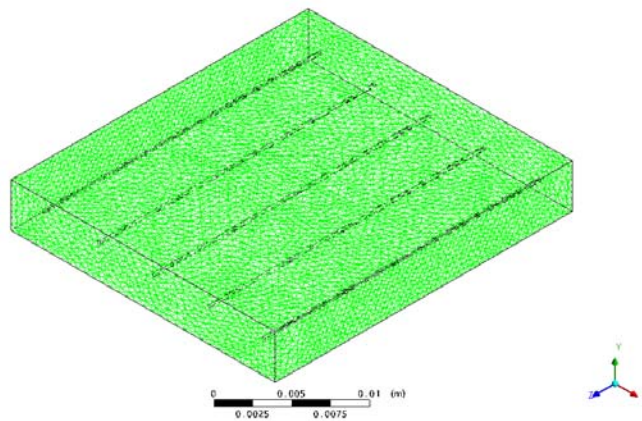


Figure 3. Volume distribution of the mesh in the SMAHC beam with Ni-Ti wires (isometric view)

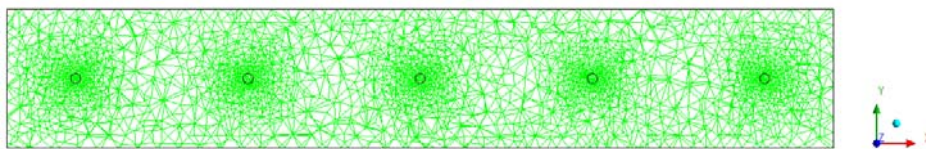


Figure 4. Cross-section distribution of the mesh in the SMAHC beam with Ni-Ti wires (XY Plane)

2.2.1. Mathematical equations

The proposed problem can be described by Eq. (2):

$$\frac{\partial \rho h_{hot}}{\partial t} - \frac{\partial p}{\partial t} + \nabla \bullet (\rho U h_{hot}) = \nabla \bullet (\lambda \nabla T) + S_E \quad (2)$$

where U is the flow velocity; S_E is the source force, ρ is the density, λ is the thermal conductivity, p is the static pressure, T is the temperature, and h_{hot} is the total enthalpy, related to the static enthalpy $h(T,P)$ by Eq. (3):

$$h_{hot} = h + \frac{1}{2} U^2 \quad (3)$$

where h is the specific static enthalpy.

3.0 RESULTS

Figure (5) show the temperature distribution for different points along of time, point 1 (x,y,z) = (8 mm, 2 mm, 130 mm), for data directly extracted in center of activation wire, and point 2 (x,y,z) = (8mm, 2.375mm, 130 mm), for data extracted immediately above of activation wire. The temperature of wire for activation 1 in point 1 reaches 71.52°C while the temperature, in point 2, for activation 2 it reaches 83.04°C. Figure (5) show that the temperature inside of wire for activation 2 is higher than activation 1.

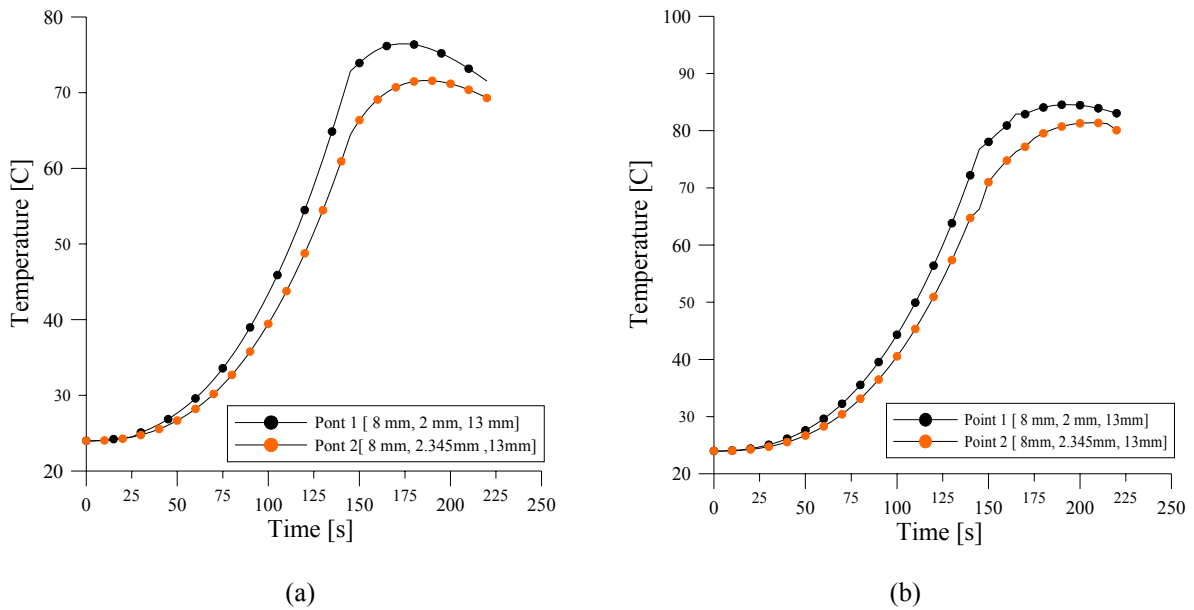


Figure 5. Temperature Distribution along of the time for two different points. (a) Activation 01. (b) Activation 02

Figure (6) presents the behavior of temperature distribution along on line $(x,y,z)=(x,2mm,130mm)$ for $t = 145s$ during heating. As can be verified in Fig. (6), for Activation 1 the temperature maximum occurs in extremity of the epoxy, while in Activation 2 its occurs in middle of the epoxy resin.

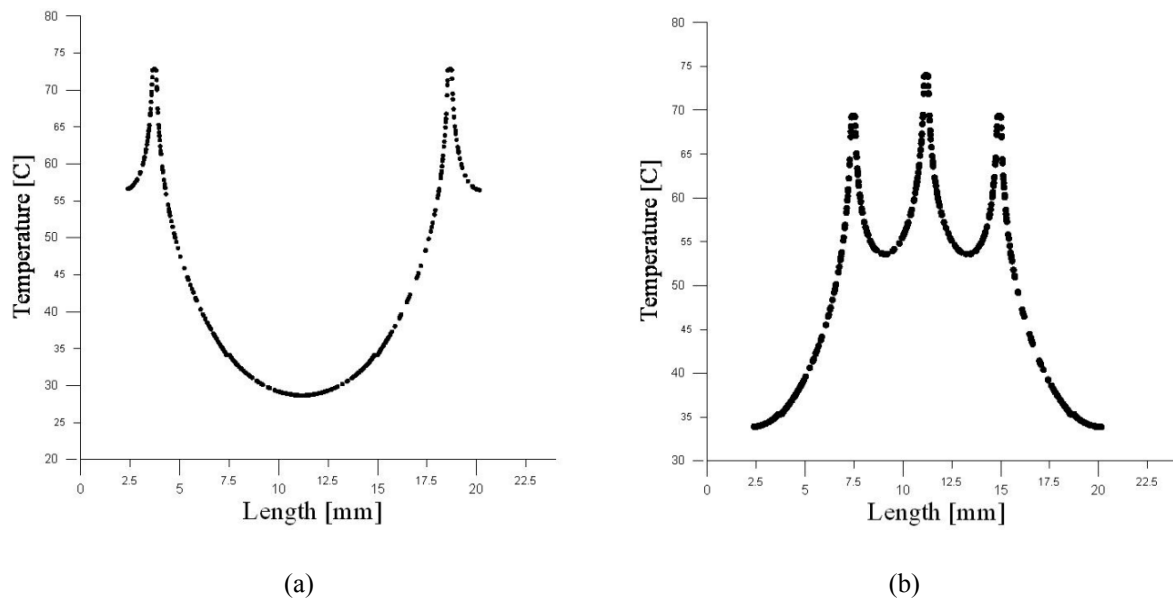


Figure 6. Temperature as a function of Length for $t = 145s$ during heating. (a) Activation 01. (b) Activation 02

The behavior of temperature distribution along the cross section of the SMAHC beam (XY plane for $z = 130 mm$) is shown in Figs. (7) and (10), through the contour lines. Figure (7) and (9) shows this thermal distribution when electrical current increases, for Activation 1 and 2, respectively, while Figs. (8) and (10) shows this behavior when electrical current decreases. As can be verified the behavior of the temperature distribution has changed with quantity of wire turned on and position of activation. Setup of the activation 2 permits one higher temperature.

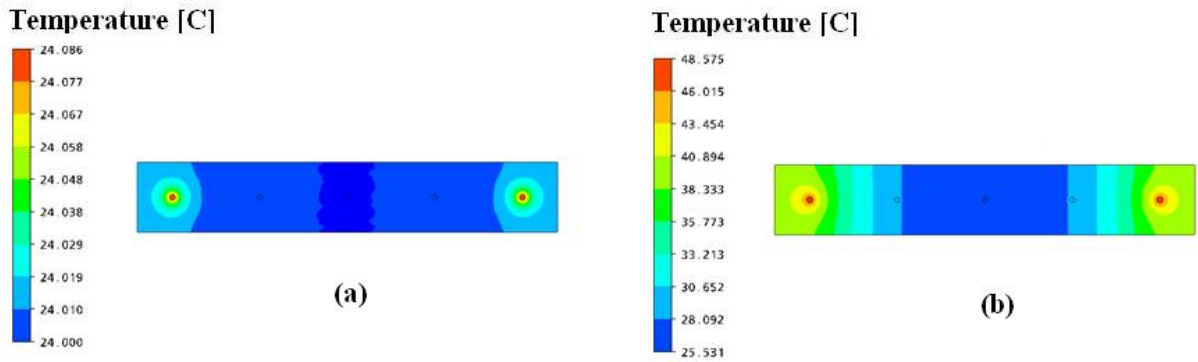


Figure 7. Activation 1 - Temperature distribution in the cross-section of the SMAHC during increase of electrical current. (a) 10 s; (b) 145 s

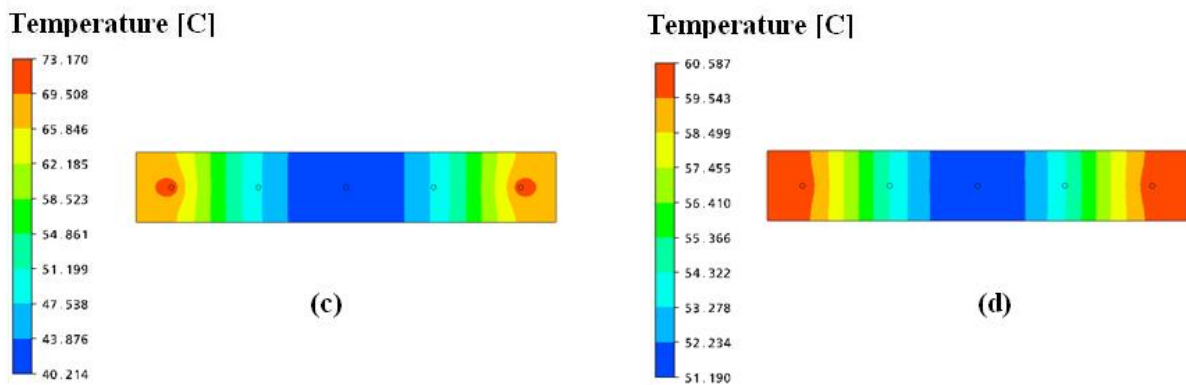


Figure 8 - Activation 1 - Temperature distribution in the cross-section of the SMAHC during reduction of electrical current. (c) 210 s (A); (d) 260 s

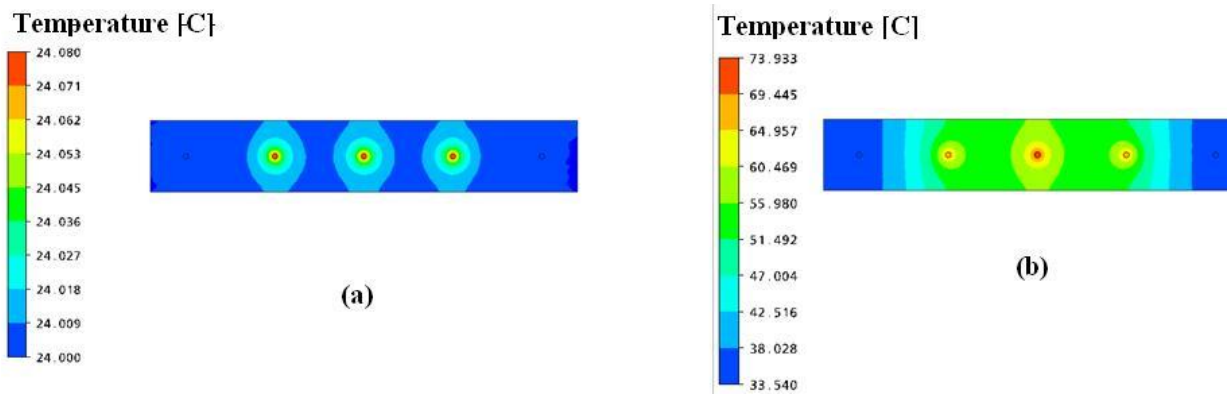


Figure 9. Activation 2 - behavior - Temperature distribution in the cross-section of the SMAHC during increase of electrical current (a) 10 s; (b) 145 s

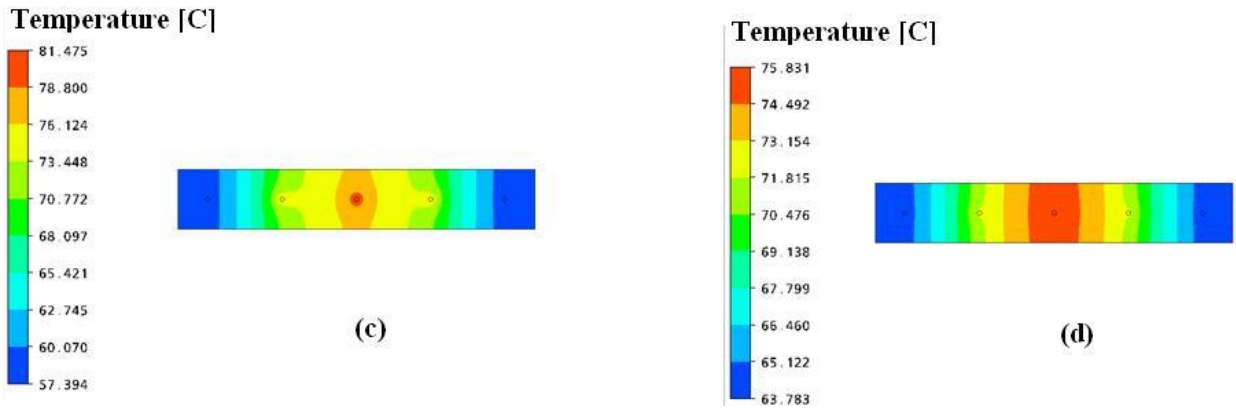


Figure 10 - Activation 2 - Temperature distribution in the cross-section of the SMAHC during reduction of electrical current. (c) 210 s ; (d) 260 s

Similar thermal behaviors are shown in Figs. (11) and (12) for the XZ plane during increase and decrease of electrical current, respectively. In these figures it is clear how activation of the Ni-Ti wire was done and how the temperature distribution along the length of the SMAHC occurs.

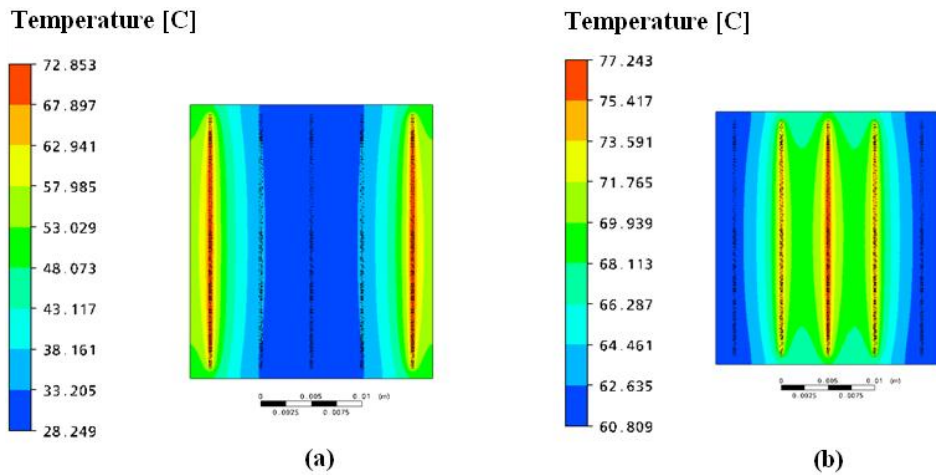


Figure 11. Temperature distribution along the XZ plane of the SMAHC during current increase ($I = 1.5 \text{ A}$). (a) Activation 1; (b) Activation 2

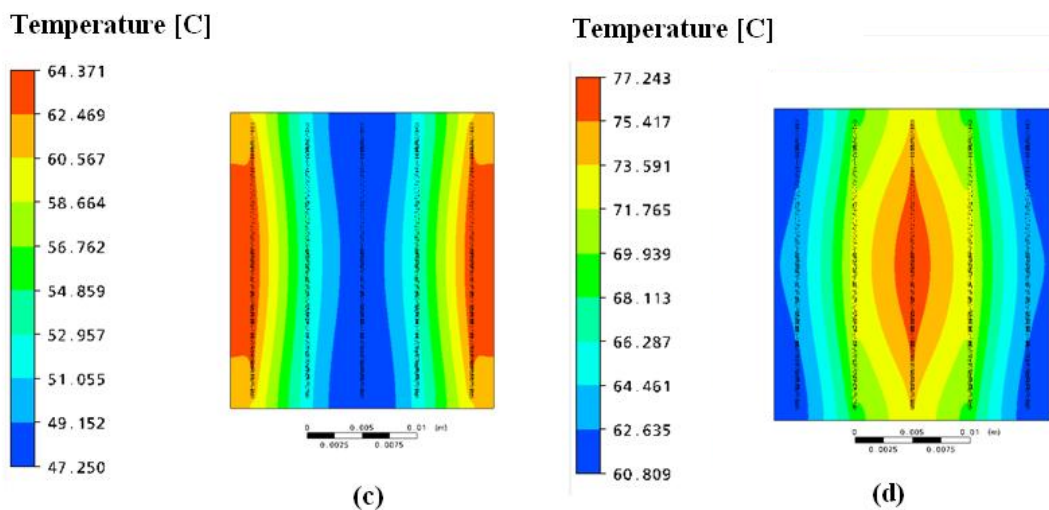


Figure 12. Temperature distribution along the XZ plane of the SMAHC during current decrease ($I = 0 \text{ A}$). (a) Activation 1; (b) Activation 2

4. CONCLUSIONS

Numerical simulation concerning the thermal distribution in the volume of a SMAHC with electrical activation of the Ni-Ti wire was consistent. The quantity of Ni-Ti wires turned on, and setup of activation had influenced on behavior the distribution temperature.

Results have presented for activation 2 showed that even with decrease of the electrical current, the temperature still had risen for much more time than Activation 1. For both activations, when the electric current decreases reaching near zero, the temperature inside of the SMAHC beam is still hot, especially inside of the Ni-Ti wires. It is precise much more than 260s for epoxy resin and wires go back to initial temperature.

5. ACKNOWLEDGEMENTS

The authors thank the Conselho Nacional de Desenvolvimento Científico e Tecnológico (CNPq), Brazilian office, for sponsoring the INCT of Smart Structures in Engineering (INCT grant 574001/2008-5) during the course of these investigations.

6. REFERENCES

- An L., Huang W.M., Fu Y.Q., Guo N.Q., 2008. "A note on size effect in actuating NiTi shape memory alloys by electrical current". *Materials & Design*, Vol.29, pp.1432-1437.
- Ashrafiuon H., Eshraghi M., and Elahinia M.H., 2006. "Position Control of a Three-link Shape Memory Alloy Actuated Robot". *Journal of Intelligent Material Systems and Structures*, Vol. 17, pp 381-392.
- Chen J., Lia Z., Zhaoc Y.Y., 2009. "A high-working-temperature CuAlMnZr shape memory alloy". *Journal of Alloys and Compounds* vol. 480, PP. 481–484.
- Frenzel J., Burow J. A., Payton E. J., Rezanka S. and Eggeler G., 2011. "Improvement of NiTi Shape Memory Actuator Performance Through Ultra-Fine Grained and Nanocrystalline Microstructures". *Advanced Engineering Materials*, Vol.12, No. 4, pp. 256–268.
- Frenzel J., Zhang Z., Neuking K., Eggeler G., 2004. "High quality vacuum induction melting of small quantities of NiTi shape memory alloys in graphite crucibles". *Journal of Alloys and Compounds*, Vol.385, pp. 214–223 .
- Huang W., 2002. "On the selection of shape memory alloys for actuators". *Materials & Design*, Vol. 23, pp.11-19.
- Humbleck J. V., 2001. "Shape Memory Alloys: A Material and a Technology". *Advanced Engineering Materials* 2001, vol. 3, No. 11. pp 837-850.
- Kang H., Wu S., Wu L., 2011. "3R and 14M martensitic transformations in as-rolled and annealed Ni64Al34.5Re1.5 shape memory alloy". *Journal of Alloys and Compounds* Vol. 509, pp. 1619–1625.
- Li Y., Rong L., Wang Z., Qi G., Wang C., 2005. "Temperature memory effect of Ti50Ni30Cu20 (at.%) alloy". *Journal of Alloys and Compounds*. Vol. 400, pp. 112–115.
- Meng X.L., Zheng Y.F., Cai W., Zhao L.C, 2004. "Two-way shape memory effect of a TiNiHf high temperature shape memory alloy". *Journal of Alloys and Compounds*. Vol. 372, pp. 180–186.
- Savi M. A., Paiva A., Bae^ta-neves A. P., Pacheco P. M. C. L., 2002. "Phenomenological Modeling and Numerical Simulation of Shape Memory Alloys: A Thermo-plastic-phase Transformation Coupled Model". *Journal of Intelligent Material Systems and Structures*, Vol. 13, pp.261-273.
- Urbina C., Flor S. De la, Ferrando F., 2010. "R-phase influence on different two-way shape memory training methods in NiTi shape memory alloys". *Journal of Alloys and Compounds*. Vol. 490, pp. 499–507.

7. RESPONSIBILITY NOTICE

The authors are the only responsible for the printed material included in this paper.